

Iron and chromium impurities in ZnSe as centers of nonradiative recombination

M. Surma and M. Godlewski

Institute of Physics, Polish Academy of Sciences, 02-668 Warsaw, Al. Lotników 32/46, Poland

T. P. Surkova

Institute of Metal Physics, Russian Academy of Sciences, Kovalevskaya 18, 620219 Ekaterinburg, GSP-170, Russia

(Received 30 March 1994)

A detailed light-induced electron-spin-resonance study of iron and chromium impurities in ZnSe is presented. The position of the Fe $2+ / 3+$ energy level in the band gap of ZnSe is determined. The role of iron and chromium impurities in nonradiative recombination processes in ZnSe is discussed.

I. INTRODUCTION

Iron, chromium, and other transition-metal (TM) impurities are some of the most common contaminants in wide-band-gap II-VI compounds. Their role in radiative and nonradiative recombination processes in these materials has been discussed for more than 50 years.¹ In ZnS, iron is known to be one of the most effective deactivators of visible luminescence.² Several processes account for this role of iron in ZnS.³ These include the so-called bypassing process (free-carrier trapping) via a deep impurity level of TM,² energy-transfer processes from donor-acceptor pairs to iron,⁴ including the three-center Auger process⁵ and formation of iron-copper pairs.⁶

In this paper we analyze the role of iron and chromium in nonradiative recombination processes in ZnSe. First, the position of the $2+ / 3+$ energy level of iron in the forbidden gap of ZnSe is determined. There is a large scatter of the data for the energy-level position of iron in the ZnSe band gap. Values ranging from about 0.75 eV,⁷ 1.1 eV,⁸ or less than 1.3 eV (Ref. 9) above the valence-band (VB) edge to 0.81 eV below the conduction-band (CB) edge¹⁰ were given. Our results explain the reason for the large discrepancy of the ionization energies reported.

The role of iron and chromium in recombination processes of electron-hole pairs is also discussed, based on the results of light-induced electron-spin resonance (photo-ESR), optically detected magnetic resonance (ODMR), photoluminescence (PL), and optical-absorption data. The results are compared to those obtained for Fe- and Cr-doped ZnS. Several nonradiative processes are shown to be important, and their relative role is analyzed.

II. EXPERIMENTAL PROCEDURE

ZnSe crystals were grown by the Bridgman technique. They were intentionally doped with iron to the level between 5×10^{16} and 4×10^{18} cm⁻³. Some reference measurements were done on chromium- and copper-doped samples doped up to 10^{19} cm⁻³.

ESR, photo-ESR, and ODMR experiments were performed on a conventional X-band ESR spectrometer.

High-pressure mercury and halogen lamps with Carl-Zeiss Jena interference filters (photo-ESR), and the 488-nm line of the Ar⁺ laser (PL, ODMR), were used for the selective optical excitation. The samples were mounted in a gas flow liquid-helium cryostat working in the temperature range 4–300 K.

III. RESULTS

Two “isotropic” (some anisotropy of the line shape was observed) ESR signals at $g = 2.044 \pm 0.001$ and 2.000 ± 0.001 were observed under and after photoexcitation at low temperatures. Based on the results of previous ESR experiments, we interpret these signals as being due to magnetic resonance of Fe³⁺ (Ref. 11) and Cr⁺,¹² respectively. They were not observed at helium temperature prior to photoexcitation.

The spectral dependencies of Fe and Cr photoexcitation were measured in the following manner. After turning on the light of the selected energy, the saturation magnitude was reached after several seconds. Then the signal intensity was measured. The next step was quenching the photoexcited signals with the second illumination of the selected energy. The latter means that the spectra shown in Figs. 1 and 2 were measured step by step for different light energies. A high-pressure mercury lamp and interference filters with high transmission were used for the selective photoexcitation and photoquenching. The experimental procedure used is common for the photo-ESR experiments¹³ but limits the resolution of the spectra obtained. The kinetics of the signal rise under illumination was also measured. A very long rise time was observed. The intensity of the Fe³⁺ ESR signal reached its stationary value at about 15 s after the light from the photoexcitation band was turned on. The spectral dependence of the rise time yields similar information to that obtained from the spectral dependence of the signal intensity.¹³

The photoexcited signals of Fe³⁺ and Cr⁺ start to decay after the light is turned off. Both time and temperature dependencies of the ESR signal decay were mea-

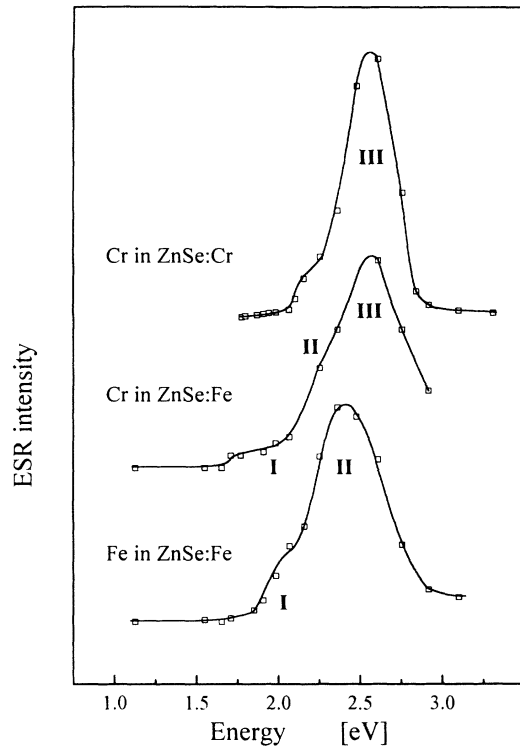


FIG. 1. Spectral dependencies of photoexcitation of Cr^+ and Fe^{3+} ESR signals in chromium- and iron-doped ZnSe. Bands I and II, as explained in the text, are due to the direct photoionization of iron (I) and chromium (II). Band III is due to the photoionization of the deep acceptor in the ZnSe lattice.

sured. A two-exponential decay was observed for the Fe ESR signal, with the second decay time (τ_2) being much longer than the first (τ_1).

At low temperature the decay time was long enough to perform the photoquenching experiments. In these experiments Fe and Cr ESR signals induced with light from the maximum of the photoexcitation bands were quenched under a second illumination of another light energy. The second illumination was switched on after the initial illumination was turned off. The obtained spectral dependence of the photoquenching of the Cr^+ ESR signal is shown in Fig. 2.

Figure 3 shows the PL spectrum of ZnSe measured for two different iron concentrations. For low Fe doping the emission is dominated by the red PL at 1.965 eV, proved by ODMR experiments to be due to the donor-acceptor pair (DAP) recombination transition. In the ODMR investigations donor and acceptor (Fig. 4) signals were observed when the detection was set at the red PL. The spectral dependence of the ODMR signal is shown in Fig. 4. The donor resonance could also be observed in the ESR for *n*-type ZnSe samples. In the infrared (Ge detector range) the 0.98- μm Fe emission was observed, identified previously as the ${}^3T_1 \rightarrow {}^5E$ transition of Fe^{2+} .^{4,8} No ODMR signal was detected via this PL band. The intensity of the red PL depends on the iron concentration in the sample, as is shown in Fig. 5.

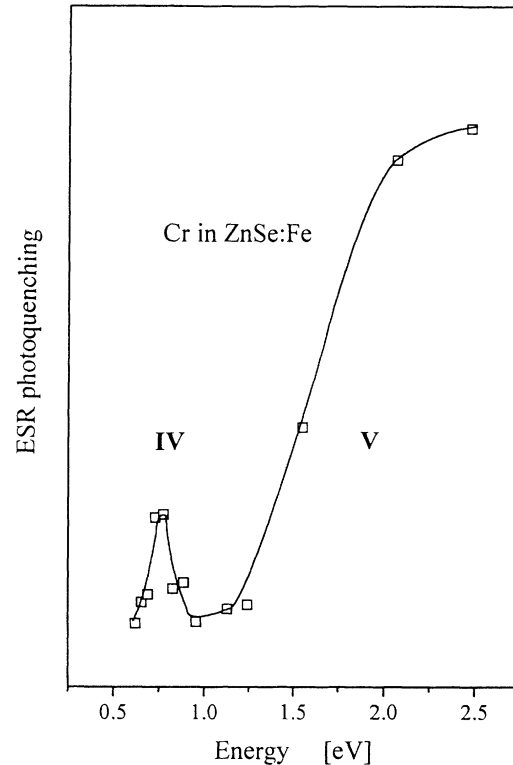


FIG. 2. Photoquenching efficiency of the Cr^+ ESR signal. Cr^+ ESR signal was induced by the initial photoexcitation. The spectrum shown describes the effect of the second illumination on the signal intensity. The experiment was performed at low temperature for which the decay time of the signal "in dark" was very long, enabling accurate photoquenching investigations.

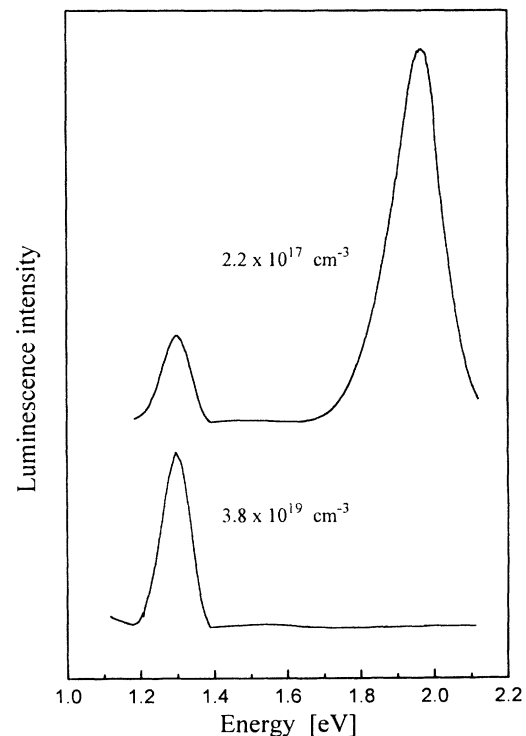


FIG. 3. Photoluminescence spectrum of ZnSe:Fe measured at the same conditions for two different iron concentrations in the sample. The spectra were detected with a Ge detector and are not corrected for the instrumental response.

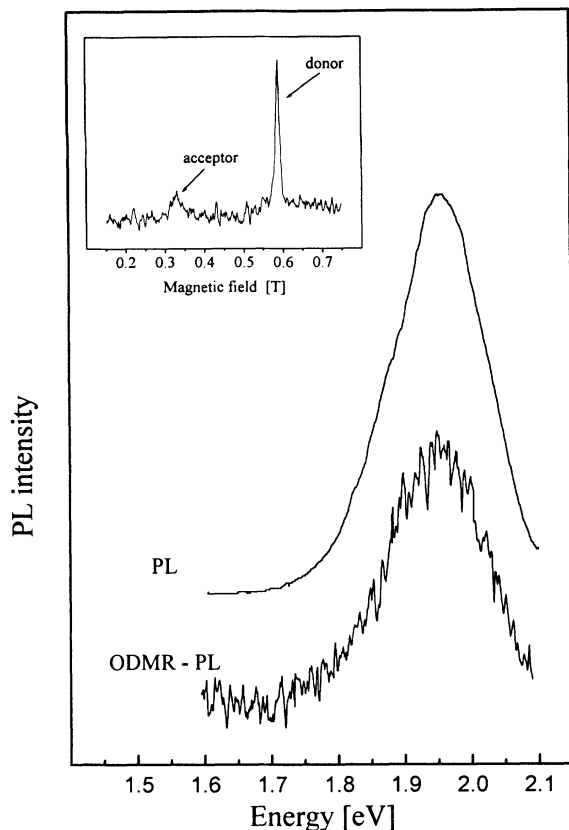


FIG. 4 Photoluminescence and spectral dependence (ODMR-PL) of the donor resonance signal observed in the ODMR experiment. The donor and rather weak and broad acceptor signals were observed in the ODMR study (see inset) for detection set at the red PL band. The latter signal was too weak to identify the origin of the acceptor center.

IV. IRON IONIZATION TRANSITIONS

Photo-ESR measurements are possible if the lifetime of the photoexcited level is longer than approximately 1 ms.¹³ For photoionization transitions to be detectable, two different processes have to be efficient. The first is the ionization transition itself, whose efficiency depends on the optical cross section for a given process. The second, often the most important, is the retrapping of the photoexcited carriers by defects other than the ionized centers. The "self-retrapping" has to be small, otherwise no photosensitivity will be observed. The latter means that other, and effective, trap centers should exist in the sample. Thus the photo-ESR experiments may help to evaluate the ionization efficiency, but they carry information about the carrier trapping as well. This is why the photo-ESR experiments are often difficult to interpret but, on other hand, may yield useful information about the overall efficiency of different recombination and trapping processes.¹³

The above is well demonstrated by the photo-ESR dependencies shown in Figs. 1 and 2. They have quite a complex nature and their explanation must be based on several complementary investigations. In our case a de-

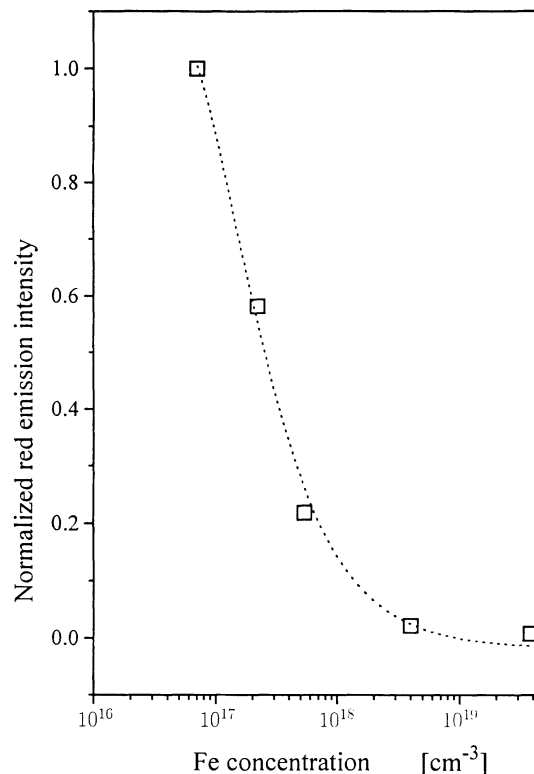


FIG. 5. Dependence of the red DAP PL intensity on iron concentration in the sample. The data were normalized to the PL intensity in the lightly iron-doped sample.

tailed knowledge of chromium ionization transitions in ZnSe (Ref. 14) helped us to interpret the observed spectra. The Cr^+ excitation spectrum in intentionally Cr-doped samples consists of two bands (II and III). Band II was shown to be due to direct chromium ionization: $\text{Cr}^{2+} \rightarrow \text{Cr}^+ + h_{\text{VB}}$, where h_{VB} denotes a hole photoexcited in the valence band (VB). Band II starts at about 1.9 eV, which is in good agreement with the previous estimations of the Cr^{2+} ionization energy.¹⁴ The second band (III) was previously shown to be due to the indirect Cr excitation process. In this process the first step is the acceptor ionization. Some of the photoexcited electrons are captured by Cr^{2+} centers. The identity of band III was verified by complementary ODMR investigations, proving the existence of the relevant acceptor centers and DAP nature of the red PL. Band III dominates even in samples which were heavily doped with Cr and which were not intentionally acceptor doped. This proves that the electron capture rate by Cr^{2+} is relatively large. Therefore Cr^{2+} ions effectively compete with shallow donors and iron centers in the electron trapping from the CB.

A different excitation spectrum is observed for samples intentionally doped with iron. Here band III is weaker than previously and an additional band (I) is observed. This band also appears in the Fe^{3+} excitation spectrum. The latter spectrum is dominated by band II, i.e., the one

due to the direct chromium ionization. Cr ionization is thus accompanied by capture of some of the photoexcited holes by Fe^{2+} centers. Coupling between indirect and direct ionization processes provides a means by which to study the latter. Here the Cr ionization process can be observed via the photosensitivity of the iron Fe^{3+} ESR signal.

When comparing Fe^{3+} and Cr^{3+} excitation spectra, we notice that the only band which can be related to Fe ionization is band I. This is why we attribute band I, at first tentatively, to the direct $\text{Fe}^{2+} \rightarrow \text{Fe}^{3+}$ photoionization. The wide spread of the previous estimations of the Fe ionization energy can be explained immediately. Band I is, in fact, much weaker than those bands due to indirect processes, which leads to the photosensitivity of the Fe^{3+} ESR signal. The present identification locates the $2+/3+$ energy level of iron at 1.1 eV above the VB edge.

The above interpretation is verified by the experimental data shown in Fig. 2. Cr^{3+} photoquenching is observed for light energies above 1.1 eV (band V), i.e., at energies for which the complementary VB iron ionization transition ($\text{Fe}^{3+} \rightarrow \text{Fe}^{2+} + h\nu_{\text{VB}}$) should occur. The Cr^{3+} ESR signal is quenched due to the hole trapping by Cr^{3+} ions. Once more, the ionization transition of one center (Fe) is best observed via the indirect photosensitivity (quenching of Cr^{3+}) of another. Even though the accuracy of the photo-ESR experiment was limited by the step by step method of obtaining the data, we could still estimate the iron ionization energy by fitting band V with the following formulas (see Ref. 13 for description of the fitting procedures and of their reliability):

$$\sigma_{\text{ion}}(h\nu) = \pi^{-1/2} \int_{-\beta}^{\infty} dz e^{-z^2} \sigma_{\text{el}}(E_{\text{opt}}, h\nu + \gamma z) \times \left[1 + \frac{\gamma z}{h\nu} \right], \quad (1)$$

where

$$\beta = \frac{(h\nu - E_{\text{opt}})}{\gamma} \quad (2)$$

and

$$\gamma = \frac{\omega_0}{\omega_{\text{ex}}} \left\{ 2(E_{\text{opt}} - E_{\text{th}}) h\omega_0 cth \left[\frac{h\omega_0}{2kT} \right] \right\}^{-1/2}. \quad (3)$$

E_{opt} and E_{th} are optical and thermal ionization energies, and their difference is called the lattice relaxation energy. ω_0 and ω_{ex} are frequencies of phonons coupled to the ground and charge excited states of the ion. For an allowed ionization transition σ_{el} may be taken as

$$\sigma_{\text{el}}(E_{\text{opt}}, h\nu) = \frac{(h\nu - E_{\text{opt}})^{1/2}}{(h\nu)^3}. \quad (4)$$

The first to the experimental data (shown in Fig. 6) gives $E_{\text{opt}} = 1.55 \pm 0.05$ eV and $E_{\text{th}} = 1.12 \pm 0.05$ eV. The reliability of the fit is presented by Fig. 6, in which theoretical curves for three different sets of ionization parameters are shown. It can be seen that within the indicated error the theoretical curves fit the experimental results.

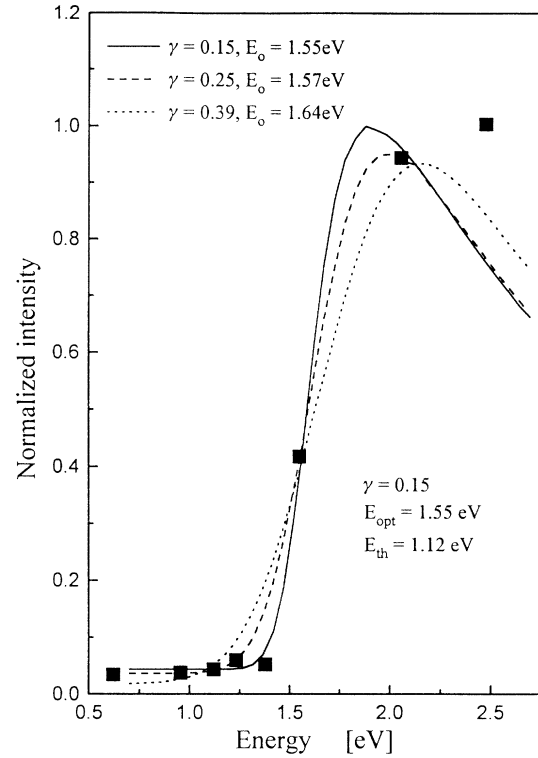


FIG. 6. Fit of the Cr^{3+} photoquenching band with the theoretical formulas described in the text. Three sets of ionization parameters are shown to demonstrate the reliability of the fit.

Band IV in the photoquenching of the Cr^{3+} ESR signal is attributed to the capture of holes generated in the VB by the photoneutralization transition of deep acceptors. The presence of these deep acceptors was proved before by both photo-ESR and ODMR investigations.

The Fe photoquenching data were less clear. After initial photoexcitation the Fe^{3+} was not totally quenched and was either decreased or enhanced by the second illumination. The appropriate ionization bands were here less distinct than those in the case of Cr^{3+} photoquenching.

Our results are consistent with the previous determination of the Cr energy level at 1.9 [1.94 (Ref. 14)] eV above the VB, and locates the Fe $2+/3+$ energy level at about 1.1 eV above the VB edge. The latter energy was determined from the photoquenching experiment since the Fe photoexcitation and optical-absorption band were too weak to perform a more detailed estimation of the ionization energy.

V. DECAY OF Cr AND Fe ESR SIGNALS IN DARK

Due to relatively long DAP recombination times, some of the pairs remain populated after the light is turned off at low temperature. This leads to the phenomenon of delayed PL and thermoluminescence (TL) in wide-band-gap II-VI compounds. TL occurs when the shallower component of the DAP (donor) is thermally ionized. The

thermally ionized carrier may be trapped by another donor, which may stimulate the DAP recombination if an occupied acceptor is close. It was observed in ZnS (Ref. 15) that some of those free electrons can be trapped by Cr^{2+} and Fe^{3+} centers which change the intensity of the relevant ESR signals. In this case, the kinetics of the ESR signal rise (Cr) or decay (Fe), and its temperature dependence yields information about the thermal ionization of carriers from shallow centers. Free carriers are trapped by the centers with relatively large cross sections. The trapping rate also depends on the relative concentration of different traps. Concluding, the ESR study can evaluate the role of a given deep center in the free-carrier capture, i.e., in the bypassing process described in Sec. I.

In ZnS, the Cr^+ ESR signal rises after the light is turned off at low temperature. This is due to the relatively large capture cross section of electrons by Cr^{2+} , which is larger than those for shallow donors and iron Fe^{3+} . Cr^{2+} thus acts as an efficient electron trap center in ZnS.⁵ This is not the case in ZnSe. A slow decay of the Cr^+ ESR signal was observed when the electrons were thermally ionized from shallow donors. The donor ionization energy is about 8 meV, as is estimated from the temperature dependence of the decay time. An explanation for this property of the Cr ESR signal will be given below.

The Fe^{3+} ESR signal decays when electrons are thermally induced to the CB. This, together with the lack of band III in Fe^{3+} photoexcitation, indicates a much larger electron trapping rate of Fe in ZnSe than in ZnS. One of the reasons for this larger cross section for electron trapping can be the different scenario of electron trapping in ZnSe. ODMR results of O'Donnell, Lee, and Watkins indicate that iron may trap an electron via the triplet (3T_1) excited state of Fe^{2+} .⁸ In ZnS the electron is trapped via the quintet state of Fe^{2+} ,⁴ i.e., a much larger energy must be dissipated by multiphonon emission. However, carrier trapping via the triplet state need not be a very efficient process. It was not confirmed by our ODMR experiment. Still our results show that the cross sections for electron and probably hole trapping by Fe in ZnSe are larger than those in ZnS. The Fe-related bypassing process should be an efficient nonradiative recombination process in ZnSe.

VI. THREE-CENTER AUGER PROCESS

The most probable explanation for the decay of the Cr^+ ESR signal in the dark is the relatively high efficiency of the three-center Auger process. The three-center Auger process was observed previously for Fe ions in ZnS.⁵ In this process DAP decays nonradiatively due to energy transfer to a nearby TM center. However, the transferred energy is not used for the TM intrashell excitation. Instead, the TM center is ionized. In ZnS the three-center Auger process was effective in the case of Fe ions and not (or less so) for Cr ions.⁵ An opposite situation occurs for Fe and Cr ions in ZnSe. The decay of the Cr^+ ESR signal when free electrons are thermally ionized

and the DAP PL is photostimulated may only be accounted for by an efficient Auger-type energy transfer from DAP to chromium, together with the rather small electron trapping rate by Cr^{2+} . This is not the case for the Fe ion in ZnSe. In ZnS the Fe^{3+} ESR signal was excited by transition III, i.e., in the indirect process starting with DAP excitation and followed by Auger-type energy transfer to iron. A lower efficiency of this process in ZnSe can be explained by a larger electron capture cross section by Fe^{3+} in ZnSe than in ZnS. No photosensitivity is observed if electrons induced to the CB are readily retrapped back by Fe^{3+} centers.

VII. NONRADIATIVE RECOMBINATION PROCESSES

Iron in ZnS is known to be an effective deactivator of visible DAP luminescence. As shown in Fig. 5, this is not the case in ZnSe crystals. A noticeable deactivation of the Cu red PL occurs for relatively large iron concentrations larger than $5 \times 10^{17} \text{ cm}^{-3}$. Four processes can account for the deactivation of the visible DAP PL in ZnSe: (1) the bypassing process; (2) the three-center Auger effect; (3) the DAP to Fe energy transfer; (4) "deep DAP" recombination involving Cr or Fe as either deep donor, or acceptor in the DAP; and (5) formation of pairs (e.g., Fe-Cu). For ZnS, the bypassing and pair formation processes were the most dominant, with the Auger effect also being active. In the case of ZnSe, the bypassing process remains dominant. The three-center Auger seems to be less effective. The DAP-Fe energy transfer, resulting in the Fe intrashell excitation, was less important in both cases. We have no definite proof that the fourth process takes place in ZnSe or ZnS. It was observed previously in, e.g., GaP in the ODMR investigations.¹⁶ The present ODMR study did not confirm the importance of such a recombination. The fifth process seems to be less important in ZnSe. In the case of ZnS the Fe-Cu pairs were detected in the ODMR.⁶ Formation of such pairs was not observed in either ESR or ODMR investigations of ZnSe:Fe. This probably explains the lower efficiency of deactivation of visible PL of ZnSe by iron.

VIII. CONCLUSIONS

The present results indicate that both iron and chromium deactivate the visible DAP emission of ZnSe. The process is less efficient than in the case of ZnS. The dominant mechanism of the PL reduction is the so-called bypassing process, with the three-center Auger transition also being important for chromium. The latter process is less efficient for iron. We have not observed the formation of Fe-Cu pairs, which may be the reason for the lower efficiency of the PL deactivation in ZnSe.

ACKNOWLEDGMENT

This work was supported by KBN Grant No. 2 0469 91 01.

- ¹N. Riehl and H. Ortman, *Z. Phy. Chem. A* **188**, 109 (1941).
- ²M. Tabei, S. Shionoya, and H. Ohmatsu, *Jpn. J. Appl. Phys.* **14**, 240 (1976).
- ³M. Godlewski and A. Zakrzewski, in *II-VI Semiconductor Compounds*, edited by M. Jain (World Scientific, Singapore, 1993), p. 205.
- ⁴M. Godlewski and M. Skowroński, *Phys. Rev. B* **32**, 4007 (1985).
- ⁵A. Zakrzewski and M. Godlewski, *Phys. Rev. B* **34**, 8993 (1986).
- ⁶M. Godlewski, W. E. Lamb, and B. C. Cavenett, *J. Phys. C* **15**, 3925 (1982).
- ⁷J. Dieleman, *Philips Res. Rep.* **20**, 206 (1965).
- ⁸K. P. O'Donnell, K. M. Lee, and G. D. Watkins, *J. Phys. C* **16**, 728 (1983).
- ⁹J. Dieleman, J. W. deJong, and T. Meijer, *J. Chem. Phys.* **45**, 3178 (1966).
- ¹⁰I. A. Gorn and A. I. Ziborov, *Works MEI* **563**, 19 (1982) (in Russian).
- ¹¹T. L. Estle and W. C. Holton, *Phys. Rev.* **150**, 159 (1966).
- ¹²R. S. Title, *Phys. Rev.* **133**, A1613 (1964).
- ¹³M. Godlewski, *Phys. Status Solidi A* **91**, 11 (1985).
- ¹⁴M. Godlewski and M. Kamińska, *J. Phys. C* **13**, 6537 (1980).
- ¹⁵M. Godlewski, *J. Appl. Phys.* **59**, 466 (1986).
- ¹⁶N. Killoran, B. C. Cavenett, M. Godlewski, T. A. Kennedy, and N. D. Wilsey, *J. Phys. C* **15**, L723 (1982).